phor analogues such as norcamphor, 5,5-difluorocamphor, pericyclocamphanone, adamantanone, adamantane, and 5,6-dehydrocamphor.[6,7] Force field and heat of formation calculations have predicted oxidation results for some of these analogues in good agreement with the experimental data.[8] We report here that cytochrome $P450_{cam}$ oxidizes a simple olefin unrelated to camphor with high stereoselectivity and independently predict the stereoselectivity of the reaction by energy minimization and molecular dynamics (MD) calculations. The remarkable agreement found between the experimental and calculated enantiomeric ratios demonstrates the potential utility of computational methods in characterizing and predicting the binding of lipophilic substrates to cytochrome P450 enzymes.

Incubation of cell-free cytochrome $P450_{cam}$ with *cis*-β-methylstyrene followed by gas–liquid chromatography (GLC) of the products[9] shows that the epoxide is formed, without loss of the cis olefin stereochemistry, at the rate of 1.3 nmol/nmol of P450 per min.[10,12] Stereochemical analysis of the epoxide metabolites was accomplished by using a chiral capillary GLC column.[13] The epoxide metabolite gives two GLC peaks which coelute with the peaks of the epoxide obtained by reaction of *cis*-β-methylstyrene and *m*-chloroperbenzoic acid. Assignment of chirality to the components of the individual peaks is based on literature data[14] and on chiral GLC correlation with a known, unequal mixture of the epoxide enantiomers provided by Dr. Thomas Kodadek.[15] Analysis of the epoxide of *cis*-β-methylstyrene produced by cytochrome $P450_{cam}$ shows that it consists of an 89:11 (±2) mixture of the 1*S*,2*R* and 1*R*,2*S* enantiomers, respectively. Cytochrome $P450_{cam}$ thus not only oxidizes *cis*-β-methylstyrene but does so with remarkable stereoselectivity.

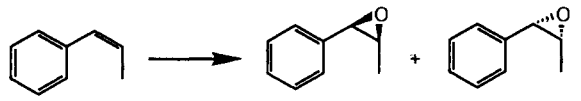

1R,2S 1S,2R

Theoretical studies using AMBER[16] to minimize enzyme–substrate orientations and molecular dynamics simulations were carried out in parallel with experimentation. The initial conformation of *cis*-β-methylstyrene, a structure with the methyl group out of the plane of the aromatic ring by about 40°, was optimized by using AMI.[17] Two separate MD simulations of 125 ps each were run for four different minimized orientations of the *cis*-β-methylstyrene docked into an extended binding site of cytochrome $P450_{cam}$.[18] Coordinates were saved every 0.2 ps, and the relative orientation of the olefin π system to the ferryl oxygen was monitored to determine the preferred face for each of these 5000 MD snapshots. Snapshots with the methyl-substituted C_β atom of the substrate farther than 4 Å from the ferryl oxygen were not counted since these distances were considered to be unreactive toward oxygen addition. The results of these simulations yield a product ratio (1*S*,2*R*/1*R*,2*S*) of 84/16, based upon the orientations of the olefin π system with respect to the putative heme-bound ferryl oxygen atom. These results lead to the prediction that the 1*S*,2*R* enantiomer should be formed in approximately 70% enantiomeric excess, a value very close to that found experimentally.

The present results indicate that cytochrome $P450_{cam}$, despite its evolutionary specificity for camphor, readily oxidizes unrelated substrates. The only real limitation on whether a compound is a substrate for cytochrome $P450_{cam}$ appears to be its size (unpublished work). The high stereospecificity of the oxidation of *cis*-β-methylstyrene, a compound with no hydrogen bonding or polar functions, must be determined primarily by contact or dispersion forces. As shown here, successful theoretical analysis of the binding of this olefin to the active site of the enzyme requires molecular dynamics simulations. The agreement between the resulting stereochemical prediction and the experimental result provides both strong support for the validity of the model and the methods used and insight into the origin of the stereoselective control of product formation.

Acknowledgment. This work was supported by National Institutes of Health Grants GM 25515 (P.O.M.) and GM 29743 (G.H.L.). Calculations were carried out at the Pittsburgh Supercomputer Center sponsored by the National Science Foundation.

(6) (a) White, R. E.; McCarthy, M.-B.; Egeberg, K. D.; Sligar, S. G. *Arch. Biochem. Biophys.* **1984**, *228*, 493. (b) Eble, K. S.; Dawson, J. H. *J. Biol. Chem.* **1984**, *259*, 14389; (c) Sligar, S. G.; Gelb, M. H.; Heimbrook, D. C. In *Microsomes, Drug Oxidations, and Drug Toxicity*; Sato, R., Kato, R., Eds.; Japan Scientific Societies Press: Tokyo, 1982; pp 155–161.

(7) During the course of this study, cytochrome $P450_{cam}$ was shown to oxidize an unrelated tetralone: Watanabe, Y.; Ishimura, Y. *J. Am. Chem. Soc.* **1989**, *111*, 410.

(8) Collins, J. R.; Loew, G. H. *J. Biol. Chem.* **1988**, *263*, 3164.

(9) GLC was done on a 0.5 mm × 30 m DB-5 column programmed to run at 35 °C for 1 min, then to rise at 70 deg/min to 80 °C, to hold at 80 °C for 3 min, and finally to rise at 2 deg/min to 150 °C. The retention times for *cis*-β-methylstyrene and its epoxide are 13.7 and 20.3 min, respectively.

(10) Incubations were carried out with cytochrome $P450_{cam}$ purified from *P. putida* essentially as reported in the literature.[11] Typical incubations (30 min at 25 °C) contained 1 μM $P450_{cam}$, 8 μM putidaredoxin, 2 μM putidaredoxin reductase, 1 mM *cis*-β-methylstyrene, and 1 mM NADH in 50 mM potassium phosphate buffer (pH 7.0).

(11) Gunsalus, I. C.; Wagner, G. C. In *Methods in Enzymology*; Fleischer, S., Packer, L., Eds.; Academic Press: New York, 1978; Vol. 52, Part C, pp 166–188.

(12) For comparison, camphor is turned over under comparable conditions at a rate of 60 nmol/nmol of P450 per min.[6a]

(13) Following extraction of the incubation mixture with 0.5 mL of hexane, the epoxide metabolite was purified prior to chiral GLC analysis by normal-phase HPLC (Alltech Partisil silica 5 μm column eluted isocratically at 1 mL/min with 2.5% tetrahydrofuran in hexane: detector at 260 nm): epoxide retention time, 8.0 min. Chiral GLC analysis was carried out on a 0.25 mm × 30 m Chiraldex G-TA capillary column (Advanced Separation Technologies, Inc.) at 120 °C. The retention times for the 1*S*,2*R* and 1*R*,2*S* *cis*-β-methylstyrene epoxide enantiomers were 9.7 and 11.9 min, respectively.

(14) Witkop, B.; Foltz, C. M. *J. Am. Chem. Soc.* **1957**, *79*, 197.

(15) O'Malley, S.; Kodadek, T. *J. Am. Chem. Soc.* **1989**, *111*, 9116.

(16) Sing, U. C.; Weiner, P. K.; Caldwell, J. W., Kollman, P. A. *AMBER UCSF Version 3.0a*; Department of Pharmaceutical Chemistry, University of California, San Francisco: San Francisco, 1986. Revision A by George Seibel (1989).

(17) Dewar, M. S. J.; Zoebisch, E. G.; Healy, E. F.; Stewart, J. J. P. *J. Am. Chem. Soc.* **1985**, *107*, 3902.

(18) The binding site consisted of 87 amino acids within ~12 Å of the Fe of the heme unit. The backbone atoms were constrained by a harmonic potential of 100 kcal/Å^2.

Structures of Proteins in Solution Derived from Homonuclear Three-Dimensional NOE-NOE Nuclear Magnetic Resonance Spectroscopy. High-Resolution Structure of Squash Trypsin Inhibitor

T. A. Holak,* J. Habazettl, H. Oschkinat, and J. Otlewski

Max-Planck-Institut für Biochemie
D-8033 Martinsried bei München, Germany

Received December 14, 1990

The nuclear Overhauser effect (NOE) is the main source of distance constraints used in the calculation of biomacromolecular structures from NMR data.[1-3] To date, distance constraints have been derived primarily from two-dimensional NOE measurements. Recently the potential of homonuclear three-dimensional NOE-NOE experiment for obtaining new types of protein connectivities has been demonstrated.[4,5] The homonuclear 3D NOE spectra should contain more information relating to distance criteria than

(1) Wüthrich, K. *NMR of Proteins & Nucleic Acids*; Wiley: New York, 1986.

(2) Kaptein, R.; Boelens, R.; Scheek, R. M.; van Gunsteren, W. F. *Biochemistry* **1988**, *27*, 5389–5395.

(3) Wagner, G. *Prog. NMR Spectrosc.* **1990**, *22*, 101–139.

0002-7863/91/1513-3196$02.50/0

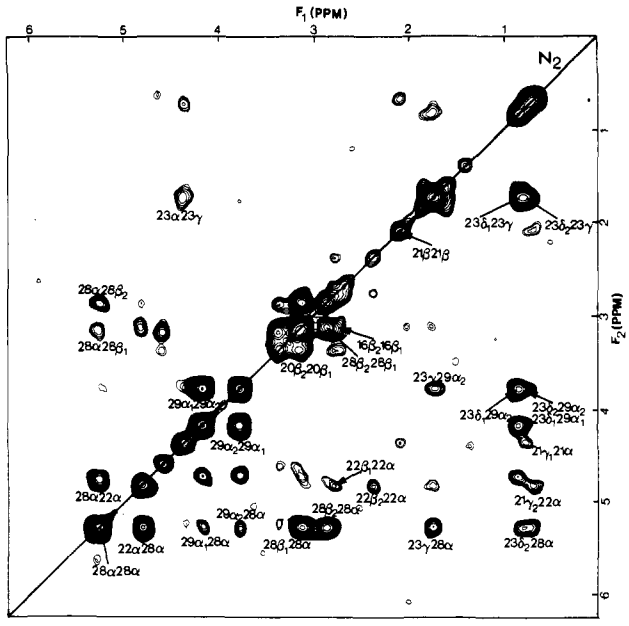

Figure 1. Cross section for F_3 at the position of the Gly29 amide proton taken from a 3D NOE-NOE spectrum of CMTI-I. NOEs at the F_1 and F_2 frequencies are labeled; the F_3 is always 29N. The homonuclear 3D NOE-NOE spectrum was acquired at 25 °C from a 9 mM sample of CMTI-I (pH 4.3 in 2 mM sodium acetate, 90% H_2O/10% D_2O) on a Bruker AMX-600 spectrometer. The experiment, carried out with use of a pulse sequence described in ref 4 had two identical mixing times of 140 ms each. Each FID consisted of 8 scans resulting in a total measurement time of 6 days. The data set consisted of $t_1 \times t_2 \times t_3 = 256 \times 256 \times 512$ points over a spectral width of 7400 Hz in all three dimensions. A subvolume containing the NH protons in F_3 only was utilized. Two regions from this subvolume were processed separately. The first subvolume comprising the region $F_1 = F_2 = 6.0$–0.0 ppm, $F_3 = 10.0$–6.4 ppm was processed with the resulting spectral data matrix of $512 \times 512 \times 1024$ points obtained after zero-filling in F_1, F_2, and F_3. Appropriate Lorentz-to-Gaussian transformations were applied together with baseline correction by a third-order polynomial fit in all 3 dimensions independently. The second region, processed similarly, comprised the portion of the spectrum $F_1 = 10.0$–0.0 ppm, $F_2 = 10.0$–0.0 ppm, and $F_3 = 10.0$–6.4 ppm.

the 2D data, which is critical for an accurate structure determination.[1-5]

This paper describes the first NMR structure determination of a small protein with use of distance constraints derived *solely from homonuclear 3D NOE-NOE spectroscopy*. The 3D data set allowed much better definition of the structures than was previously possible in the 2D spectra. The solution structure of squash trypsin inhibitor (CMTI-I) was recently determined from NMR data based on various two-dimensional spectra.[6] These structures were based already on a very large number of distance constraints (324 interproton distance constraints for 29 residues). A *single* homonuclear 3D NOE-NOE experiment in water provided every NOE previously observed in two 2D NOESY spectra measured in H_2O and D_2O. In addition 217 nontrivial distance constraints were determined from the 3D NOE-NOE spectrum which could not be obtained from these two 2D NOESY spectra. The current structures are thus based on 541 distance constraints (19 distance constraints per residue).

The intensity of the 3D NOE-NOE cross-peak, a_{ijk}, is proportional to the product of the individual NOE transfer efficiencies of each mixing time.[4,7,8] In a second-order approximation for τ_m and with both mixing times equal, the intensity of the 3D NOE-NOE cross-peak is proportional to

$$a_{ijk} \approx a_{ij}a_{jk} = \sigma_{ij}\sigma_{jk}\tau_m^2 = Kr_{ij}^{-6}r_{jk}^{-6}$$

where σ_{ij} is the cross-relaxation rate between spins i and j, τ_m is the mixing time, K is the proportionality constant, and r_{ij} is the interproton distance constraint. The back-transfer peak B, a_{iji},[5] is then proportional to the square of the cross-relaxation rate σ_{ij}. It can be shown that in contrast to 2D NOESY there is no contribution to a_{ijk} and a_{iji} from spin diffusion terms of second order for spins other than i, j, and k; however, indirect transfers of third and higher order in τ_m are still present in these peaks (since the 3D peak itself is second order in τ_m the relative contributions of spin diffusion are similar in 2D and 3D cross-peaks). For the N_1 and N_2 peaks,[5] a_{ijj} and a_{iij}, respectively, the intensity a_{ijj} or a_{iij} is directly proportional to r_{ij}^{-6}, $a_{ijj} \propto \sigma_{ij}\tau_m$, assuming that only the first-order term is retained in the linear approximation for τ_m. The N_1 and N_2 cross-peaks are due to the direct NOEs during the first and second mixing times, respectively.[5]

The 3D cross-peak intensities were semiquantified by measuring the intensity of the highest point in a volume around the 3D cross-peak. This intensity is directly proportional to the volume of the 3D cross-peak provided that the line width of every peak in all 3 dimensions is similar and larger than multiplicities of the signals. This is the case in the 3D NOE-NOE spectrum. The distance constraints involved in the 3D NOE-NOE cross-peaks were extracted in the following manner. Three separate calibration constants (K's) were determined by using the connectivities which involved known interproton distances: two constants for the cross peaks with two of the three frequencies equal (the N_1, N_2, and B cross-peaks), and the other for "real" 3D NOE-NOE cross-peaks with three different frequencies. The calibration constants for the N_1 and N_2 (and also B) peaks can be used directly to estimate distance constraints from the experimental intensities on these lines. For example, the N_2 connectivity 28α-28α-29N in Figure 1 gives the distance constraint between Cys28C$^\alpha$H and Gly29-HN (the notation 28α-28α-29N corresponds to the cross-peak [F_1 = Cys28C$^\alpha$H] – [F_2 = Cys28C$^\alpha$H] – [F_3 = Gly29HN] on the N_2 line at the NH amide plane of residue Gly29). For the 3D cross-peaks with three different frequencies, the distance constraint corresponding to one of the two NOE transfers has to be known in order to calculate the distance constraint involved in the other transfer. These reference distance constraints were acquired from the distance constraints obtained from the N_1 and N_2 cross-peaks. The interproton distances derived from known amino acid geometries were also used.[1,9-11]

Once an initial set of distance constraints was established, they were used to calculate other interproton distance constraints involved in the 3D NOE-NOE transfers. In many cases one distance constraint could be calculated from several different 3D cross-peaks; for example, the connectivity 22C$^\alpha$H-28C$^\alpha$H (Figure 1) was found in the four NH planes 22α-28α-29N, 22α-28α-21N, 22α-28α-28N, and 22α-28α-23N. In cases such as the connectivity 22α-28α, only one distance constraint was entered into the input table, usually the one involved in the strongest cross-peak. There was usually little deviation among the distance constraints derived from different cross-peaks. The distance constraints were entered as equilibrium values obtained from the calibrations with bounds ±0.5 Å for distance constraints of 2.3–3.5 Å and ±0.8 Å for distances between 3.6 and 4.3 Å, respectively.

Thirty structures were calculated with use of the basic protocol presented previously.[6] The structures, shown in Figure 2, exhibit very small deviations from idealized covalent geometry and energies which are similar to those published previously. All structures satisfy the experimental constraints. There are no

(4) Boelens, R.; Vuister, G. W.; Koning, T. M. G.; Kaptein, R. *J. Am. Chem. Soc.* **1989**, *111*, 8525–8526.
(5) Breg, J. N.; Boelens, R.; Vuister, G. W.; Kaptein, R. *J. Magn. Reson.* **1990**, *87*, 646–651.
(6) Holak, T. A.; Gondol, D.; Otlewski, J.; Wilusz, T. *J. Mol. Biol.* **1989**, *210*, 635–648.
(7) Griesinger, C.; Sørensen, O. W.; Ernst, R. R. *J. Magn. Reson.* **1989**, *84*, 14–63.
(8) Oschkinat, H.; Cieslar, C.; Griesinger, C. *J. Magn. Reson.* **1990**, *86*, 453–469.
(9) Wüthrich, K.; Billeter, M.; Braun, W. *J. Mol. Biol.* **1984**, *180*, 715–740.
(10) Kline, A.; Braun, W.; Wüthrich, K. *J. Mol. Biol.* **1988**, *204*, 657–672.
(11) Williamson, M. P.; Havel, T. F.; Wüthrich, K. *J. Mol. Biol.* **1985**, *82*, 295–315.

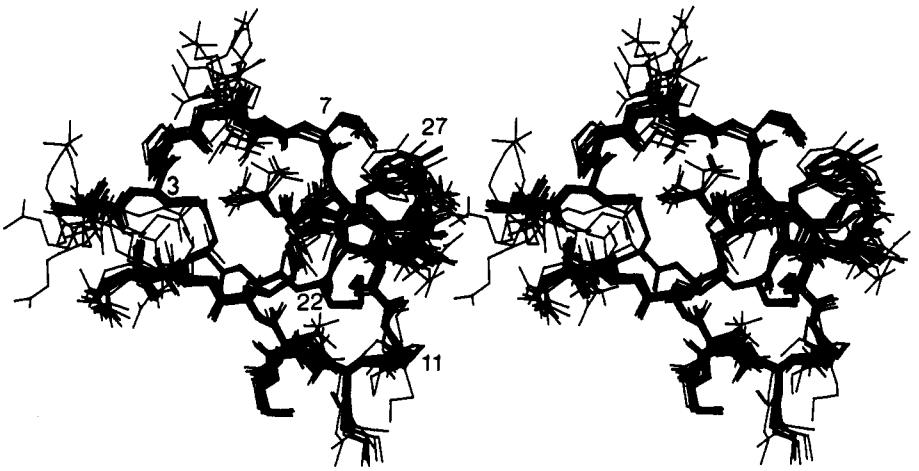

Figure 2. Best superposition of the backbone (N, C^{α}, C, O; residues 2–29) of the 12 structures. All heavy atoms are shown. The average of the root-mean-square differences among the 3D NOE-NOE structures is 0.51 ± 0.11 Å for the backbone atoms and 1.18 ± 0.13 Å for all heavy atoms.

distance constraint violations greater than 0.5 Å. The root-mean-square difference from the experimental constraints, which are calculated with respect to the upper and lower limits of the distance constraints,[6] is 0.060 ± 0.008 Å for all 541 distance constraints. When the new structures are checked for distance constraint violations against the 324 2D NOESY distance constraints (with the upper and lower bounds to distance constraints used in the present study), the root-mean-square difference is 0.081 ± 0.010 Å. The root-mean-square difference is lower than that for the 2D NOESY distance constraints while the number of NOEs is 65% greater for the new structures.

In one set of 12 structures, the disulfide bridges were defined neither as bonds nor as distance constraints. These structures were almost identical with those calculated with the disulfide bonds specified. The S–S pairing could be determined unambiguously from the NMR structures. Also, in contrast to the previous structures, the present structures exhibit unique conformations for all the disulfide bridges. The ability to obtain structures with the uniquely determined conformations of the disulfide bridges could be traced to the presence of new NOEs in the 3D spectrum involving cysteines.

In conclusion, we have shown that a single 3D NOE-NOE experiment of a protein in water can provide sufficient input data to calculate structures that could be deemed to correspond to high-resolution structures as defined in X-ray crystallography. A large number of NOEs can be extracted from the homonuclear 3D spectrum, together with NOEs not observed in 2D NOESY spectra. This is especially true for connectivities between the side-chain protons of different residues. Around 200 such long-range NOEs could be obtained from the 3D NOE-NOE spectrum. For the 2D spectrum, the aliphatic region of the NOESY spectrum is used to extract such connectivities; due to experimental limitations,[1] this requires a spectrum of protein dissolved in D_2O. In the 3D NOE-NOE spectrum in H_2O, the NOEs between the aliphatic protons can be observed at unique amide proton frequencies. It is also easier to assign such connectivities in the 3D than the 2D spectrum because of the possibility of multiple checking of the assignments due to the redundancy and mutual consistency of the 3D cross-peaks. Since 3D NOE-NOE spectroscopy does not rely on coherent transfers due to the scalar coupling, its sensitivity is not restricted by small J coupling or large line widths. The 3D NOE-NOE spectroscopy should therefore be useful in the structure determination of large biomolecules. Of course, the method is not limited to biomolecules; it should be useful for any organic compounds that give rise to the NOE effect. We expect that the homonuclear 3D NOE-NOE spectroscopy will replace or supplement the 2D NOESY for structure determination.

Acknowledgment. This work was supported by a research grant from the Bundesministerium für Forschung und Technologie (Grant No. 0318909A). J.O. is a recipient of a fellowship from the Humboldt Foundation.

Supplementary Material Available: Figure giving the F_3 NH cross section at amide of residues 22 and 8 and tables containing angle and distance constraints used in the calculations together with the 3D connectivities involved in these distance constraints (20 pages). Ordering information is given on any current masthead page. Tables containing constraints and coordinates of the five structures have been also deposited in the Brookhaven Protein Data Bank.

Isolation and Structure Elucidation of the 4-Amino-4-deoxychorismate Intermediate in the PABA# Enzymatic Pathway

Karen S. Anderson,*,† Warren M. Kati,† Qi-Zhuang Ye,‡,§ Jun Liu,‡,∥ Christopher T. Walsh,‡ Alan J. Benesi,⊥ and Kenneth A. Johnson†

Department of Molecular and Cell Biology
The Pennsylvania State University
University Park, Pennsylvania 16802
Department of Biological Chemistry &
Molecular Pharmacology
Harvard Medical School, Boston, Massachusetts 02115
Department of Chemistry
The Pennsylvania State University
University Park, Pennsylvania 16802

Received December 17, 1990

PABA (*p*-aminobenzoic acid), an important precursor in the bacterial biosynthetic pathway for folate coenzymes, is formed

* Author to whom correspondence should be addressed. Present address: Yale Medical School, 333 Cedar St., New Haven, CT 06150.
† Department of Molecular and Cell Biology, The Pennsylvania State University.
‡ Department of Biological Chemistry & Molecular Pharmacology, Harvard Medical School.
§ Present address: Parke-Davis Pharmaceutical Research, 2800 Plymouth Rd., Ann Arbor, MI 48105.
∥ Present address: Harvard University, Department of Chemistry, 12 Oxford St., Cambridge, MA 02138.
⊥ Department of Chemistry, The Pennsylvania State University.
Abbreviations used: PABA, *p*-aminobenzoic acid; TRIS, tris(hydroxymethyl)aminomethane; PabA, PABA synthase subunit having glutaminase activity; PabB, PABA synthase subunit having aminodeoxychorismate synthase activity; PabC, PABA synthase subunit having aminodeoxychorismate lyase activity, formerly referred to as enzyme X.

0002-7863/91/1513-3198$02.50/0